INFRASOUND SIGNALS FROM GROUND-MOTION SOURCES

Rodney W. Whitaker

Los Alamos National Laboratory

ABSTRACT

This report presents progress on an ongoing research project looking at near-field infrasound signals as a basis for discriminants between underground nuclear tests (UGT) and earthquakes (EQ). In an earlier program, infrasound signals from UGTs and EQs were collected at ranges of a few hundred kilometers, in the far-field. Analysis of these data revealed two parameters that had potential for discrimination purposes: signal duration and wind-corrected amplitudes. These far-field differences should be present in the near-field signals as well. To study the near-field signals, we are using computational techniques based on modeled ground motions from UGTs and EQs. One is the closed form numerical integration of the Rayleigh integral (RI), and the other is the application of a time-domain, finite-difference computational fluid dynamics (CFD) program, CAVEAT. This report summarizes recent progress in modeling these signals, showing comparisons of waveforms and power spectra from the two techniques. There is also a discussion of the effects of spatial and temporal zoning on the quality of the results. Application of Fourier techniques to the basic ground models is introduced as an analytic path to the radiation patterns of the ground-motion sources.

Report Documentation Page		*Form Approved* *OMB No. 0704-0188*

Public reporting burden for the collection of information is estimated to average 1 hour per response, including the time for reviewing instructions, searching existing data sources, gathering and maintaining the data needed, and completing and reviewing the collection of information. Send comments regarding this burden estimate or any other aspect of this collection of information, including suggestions for reducing this burden, to Washington Headquarters Services, Directorate for Information Operations and Reports, 1215 Jefferson Davis Highway, Suite 1204, Arlington VA 22202-4302. Respondents should be aware that notwithstanding any other provision of law, no person shall be subject to a penalty for failing to comply with a collection of information if it does not display a currently valid OMB control number.

1. REPORT DATE **SEP 2008**	2. REPORT TYPE	3. DATES COVERED **00-00-2008 to 00-00-2008**
4. TITLE AND SUBTITLE **Infrasound Signals from Ground-Motion Sources**		5a. CONTRACT NUMBER
		5b. GRANT NUMBER
		5c. PROGRAM ELEMENT NUMBER
6. AUTHOR(S)		5d. PROJECT NUMBER
		5e. TASK NUMBER
		5f. WORK UNIT NUMBER
7. PERFORMING ORGANIZATION NAME(S) AND ADDRESS(ES) **Los AlamosNational Laboratory,PO Box 1663,Los Alamos,NM,87545**		8. PERFORMING ORGANIZATION REPORT NUMBER
9. SPONSORING/MONITORING AGENCY NAME(S) AND ADDRESS(ES)		10. SPONSOR/MONITOR'S ACRONYM(S)
		11. SPONSOR/MONITOR'S REPORT NUMBER(S)

12. DISTRIBUTION/AVAILABILITY STATEMENT **Approved for public release; distribution unlimited**

13. SUPPLEMENTARY NOTES **Proceedings of the 30th Monitoring Research Review: Ground-Based Nuclear Explosion Monitoring Technologies, 23-25 Sep 2008, Portsmouth, VA sponsored by the National Nuclear Security Administration (NNSA) and the Air Force Research Laboratory (AFRL)**

14. ABSTRACT **see report**

15. SUBJECT TERMS

16. SECURITY CLASSIFICATION OF:			17. LIMITATION OF ABSTRACT	18. NUMBER OF PAGES	19a. NAME OF RESPONSIBLE PERSON
a. REPORT **unclassified**	b. ABSTRACT **unclassified**	c. THIS PAGE **unclassified**	**Same as Report (SAR)**	**9**	

Standard Form 298 (Rev. 8-98)
Prescribed by ANSI Std Z39-18

OBJECTIVES

The objective of this research is to find differences in the near-field infrasound signals of UGTs and earthquakes that can be the basis for establishing discriminants between the two sources. Such differences in the near-field signal would likely survive to a longer range.

RESEARCH ACCOMPLISHED

We have continued the numerical studies on modeling the near-field infrasound signal from the surface ground motion from underground nuclear tests (UGT) and earthquakes (EQ). The computational tools include numerical integration of the closed-form RI and the use of the time-domain, finite-difference code CAVEAT. CAVEAT was only mentioned in last year's MRR report but has been used more extensively this past year.

CAVEAT Developments

CAVEAT is an established computational tool and has been applied to calculations of the time evolution of atmospheric nuclear explosions, including hydrodynamic outputs and optical signature outputs. CAVEAT is documented in Adessio et al. (1992). The following succinct description of the CAVEAT code is directly quoted from the abstract of the Adessio et al. (1992) report:

> CAVEAT uses an explicit time-marching, conservative finite-volume numerical technique in which all state variables, including velocity, are cell centered; values at vertices and cell faces are derived. The technique is a variation of the Godunov method that uses an approximate Riemann solver and accommodates arbitrary equations of state. Spatial differencing may either be first order (constant across the cell) or second order (linear variation across the cell) with a choice of limiters of the gradient in an attempt to preserve monotonicity. The formulation is spatially two-dimensional with options for Cartesian and curvilinear geometries, e.g., cylindrical (r,z). Discretization is achieved with a mesh of arbitrary quadrilateral cells whose vertices can move with time. Arbitrary mesh motion is supported by allowing transport of material between cells according to the arbitrary Lagrangian-Eulerian (ALE) technique. The computation is performed in two phases: a Lagrangian phase and a remapping phase in which conserved variables are transferred from the Lagrangian mesh to an arbitrary specified mesh. The dynamic mesh capability generally smoothes distortions in the mesh and can also result in higher resolution around features of interest, such as a shock discontinuity.

The report contains results for test cases of a shock tube, spherical blast wave, a pure advection problem, and a shock on wedge.

The initial calculations with CAVEAT used a separate ground motion acceleration model that was not the same as that used in the RI code. We have worked to correct this by using bi-cubic spline interpolations on the RI code computed velocity data as a function of range, r, and time, t. For a given event, the full set of surface velocities, $v(r,t)$ is written to an input file to CAVEAT. At the bottom of the CAVEAT mesh (grid), we employ the specified velocity boundary condition whose values at a specific time and range are interpolated from the $v(r,t)$ field using the bi-cubic spline algorithms from Press et al. (1990). In this manner the velocity data in the RI code and in CAVEAT can be made nearly the same. This scheme is quite general and efficient and applicable to other ground motion sources as well.

For the CAVEAT results reported here, we used cylindrical (r,z) coordinates with 500 mesh cells in each direction. The standard run was with radial and vertical steps of 30 m. The finer zone calculation was performed with mesh sizes of 15 m. The runs were made with an ALE coefficient of 0.9. The ambient atmosphere was from a Committee on Space Research (COSPAR) International Reference Atmosphere (CIRA) standard atmosphere.

We first show pressure contours for the standard and fine zone calculation (Figure 1), where the input velocity data were from the modeled accelerations for the Tortugas event in hole U3gg. In the CAVEAT results, we show the signal pressure that is the total pressure minus the ambient pressure, sometimes referred to as the perturbation pressure.
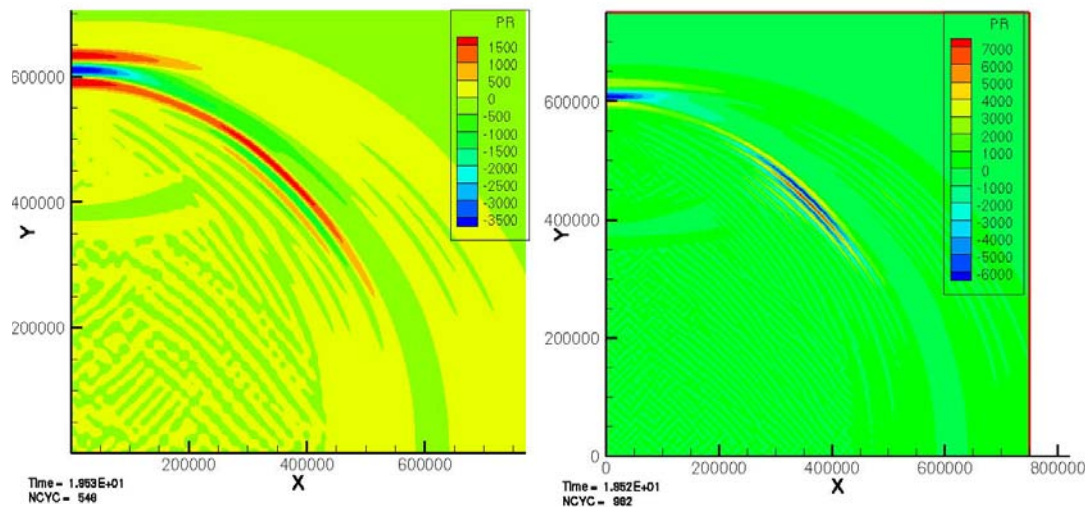
Figure 1. Pressure contours for the standard CAVEAT run (left) and finer zone calculation (right) at 20 seconds. The x and y values are in centimeters, and pressure contours are in dynes/cm^2. Each calculation used 250,000 zones. Pressure contour values are shown in the upper right.

The finer zone result shows more structure in the pressure field. From the contour legends we see that the finer zone result has larger (in absolute value) maximum and minimum pressures. By taking radial slices through the mesh at different elevation angles we can make additional comparisons. An example is shown in Figure 2.

A   B
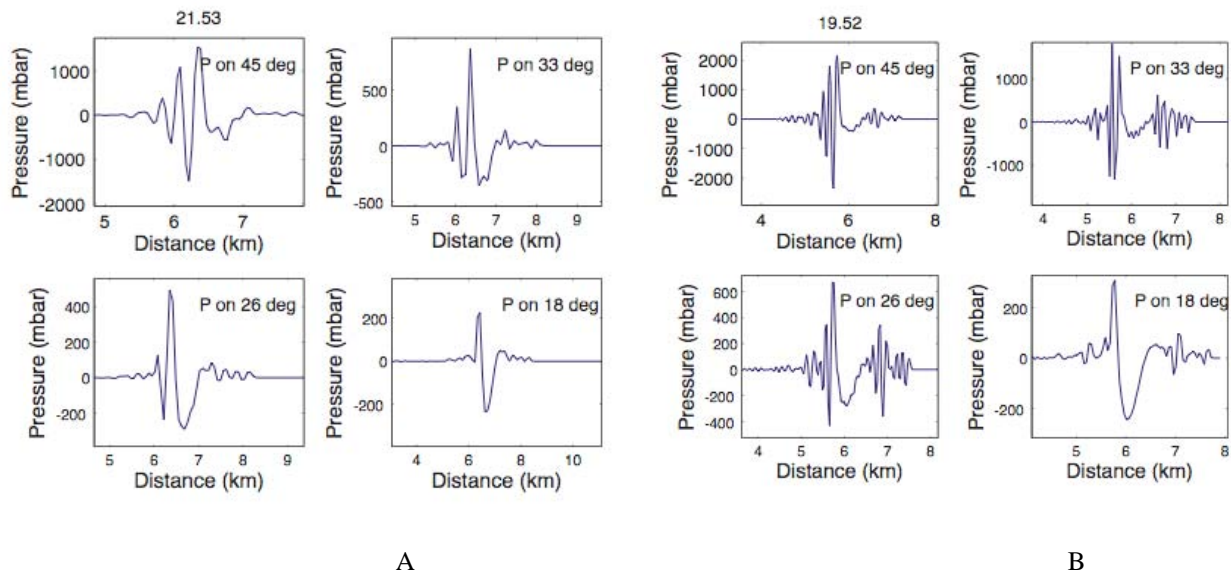
Figure 2. Radial slices through the Caveat mesh for the standard run (left 2 × 2 set, A) and for the finer zone run (right 2 × 2 set, B). The slices are at elevation angles of 18, 26, 33, and 45 degrees. The pressure unit "mbar" stands for "micro bar."

The finer zone run generally has higher frequency structure and larger amplitudes, compare the 33-degree panels. To examine the impact of smoothing, we did a five-point running average on the pressure values on the 45-degree fine zone data (B set), and the result is quite similar to the 45-degree standard run result (A set). These results show the improved velocity model that has now been implemented into CAVEAT.

Rayleigh Integral (RI) Code Developments

For review, the RI is given by the following equation:

$$p(R_0, t) = \frac{\rho}{2\pi} \int \frac{a(r, (t - R/c))}{R} dA_s \,, \tag{1}$$

where a is the acceleration of the ground, r is a location on the ground (referenced to a center position), dA_S is an element of area on the ground, R is the distance from the ground element to the observing point, t is time, ρ is the air density, c is the speed of sound in air, p is the air pressure, and R_0 is the observation location.

The RI code uses modeled ground motions for some 30 events. The parameters include the peak acceleration and temporal width of the initial acceleration pulse and the same for additional contributions from plastic or cavity rebound signals. A specified exponential decay with range is also applied.
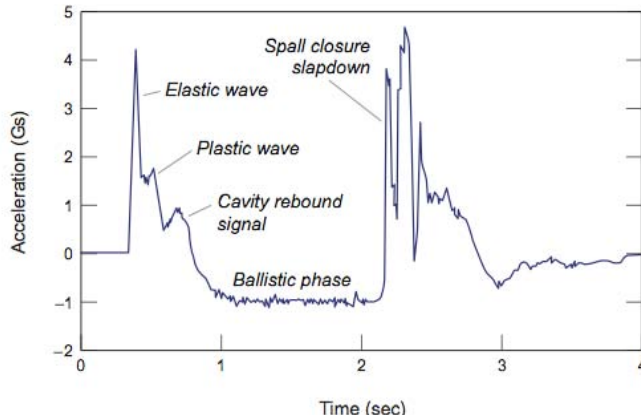

Figure 3 illustrates the features in UGT acceleration records. Some events have just the initial and slapdown contributions, such as Tortugas, U3gg, while others have additional contributions such as Duoro, U3lv. When the acceleration is the simple two-pulse shape, the velocity exhibits a simple form as well. This is illustrated in Figure 4. The acceleration is a classic two-pulse record, and the velocity has a well-defined linear portion due to the –1 g spall phase in the acceleration, Jones et al. (1993) and Huan and Walker (1980).

Figure 3. An illustration of the characteristics of ground motion from a UGT.
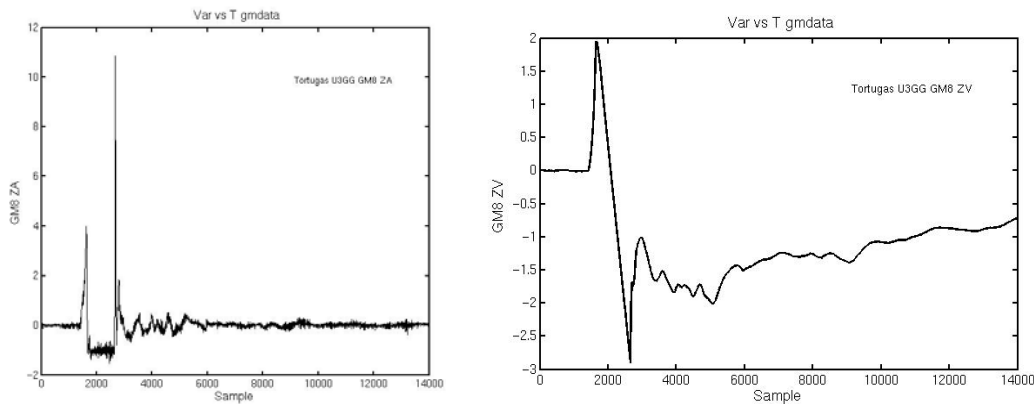

Figure 4. A measured ground-motion acceleration record for Totugas (left) and the velocity record (right), where units are gs for acceleration and m/s for velocity. The horizontal axis is the sample number.

If the acceleration record has contributions from other components, the behavior is more complicated, as is illustrated in Figure 5 for the Duoro event.
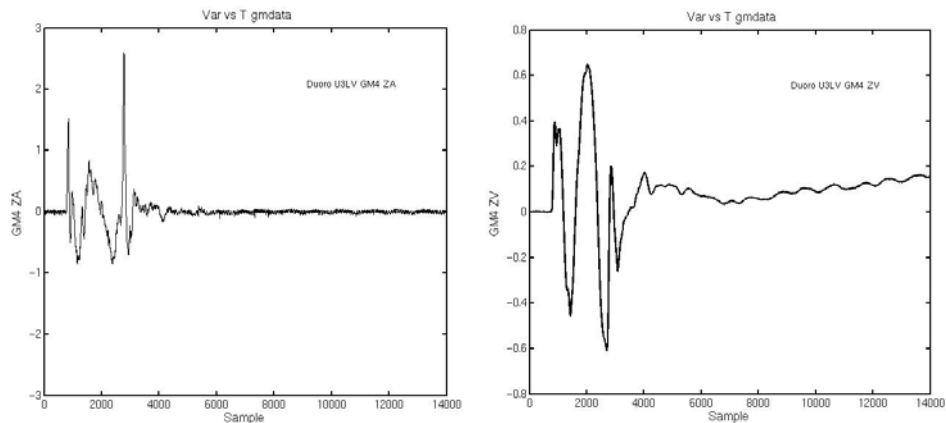
Figure 5. The same as Figure 4 except for the Duoro event, which shows more-complicated behavior.

We use the modeled ground motions from these two events to illustrate some results from the RI code. First, we show computed power spectra for the RI code calculation for an observer at an horizontal range of 5 km and a height of 4 km and for an observer at a horizontal range of 15 km and a height of 10 km. These are close to the same elevation angle. Figure 6 presents this comparison and shows good agreement.
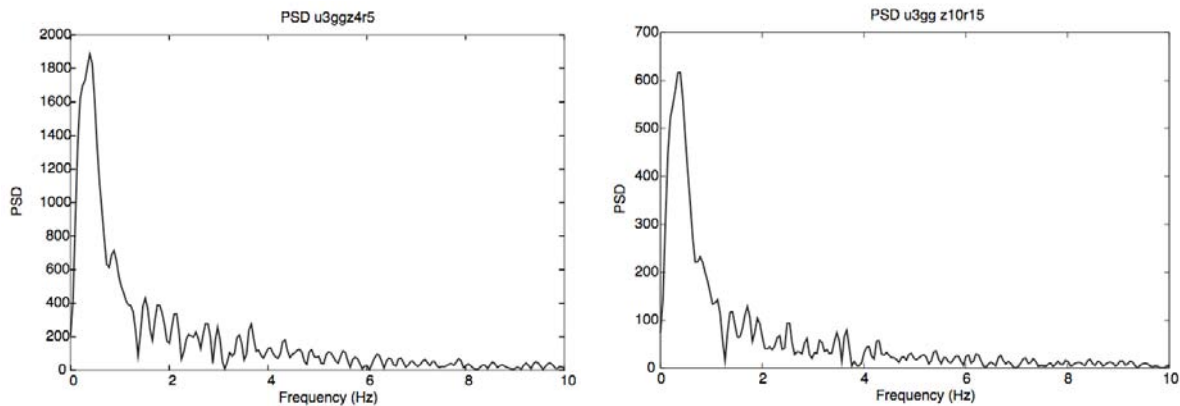

Figure 6. Power spectra (relative units) for the Tortugas event, hole U3gg, for a height of 4km and a range of 5 km (left) and for a height of 10 km and range of 15 km (right). The results are reassuringly close. Frequency is on the horizontal axis.

To illustrate the effects of the more complicated ground motion, Figure 7 shows the RI code power spectra for the Duoro event. As expected, the Duoro event has larger contributions at higher frequencies than does the Tortugas event, due to the more-complicated source acceleration.
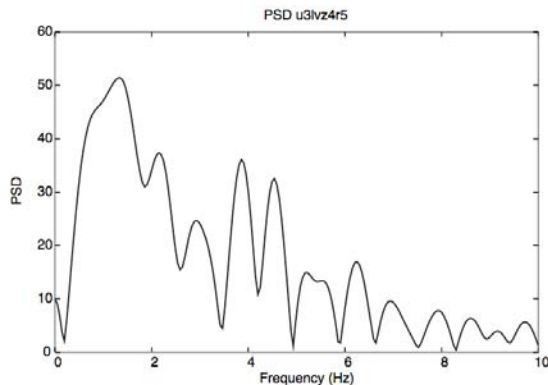
Figure 7. RI code power spectra (relative units) for the Duoro event at a range of 5 km and a height of 4 km. Frequency is on the horizontal axis. Compare this result with that in the left panel of Figure 6.

Initial Comparisons of Two Techniques

Below we show a comparison between the CAVEAT and RI codes for the Tortugas event, U3gg. CAVEAT advances in time so that, at a given time, we can take a snapshot of the pressure field in the computational domain. Then we can plot radial slices through that domain at different elevation angles. This is shown in Figure 8 with the left four plots from CAVEAT. The RI code provides a time history at a given observation location. When looking at the CAVEAT radial slices, one must remember that the pulse is proceeding to the right. Thus to properly compare the two code results one should flip the CAVEAT plot. With that in mind, one can see that the waveforms are quite similar in shape. The RI code result is at 45 degrees and shows a little better agreement with the CAVEAT profile at 26 or 18 degrees. This is probably due to refraction in a layered atmosphere as is used in CAVEAT while a uniform atmosphere is used in the RI code.
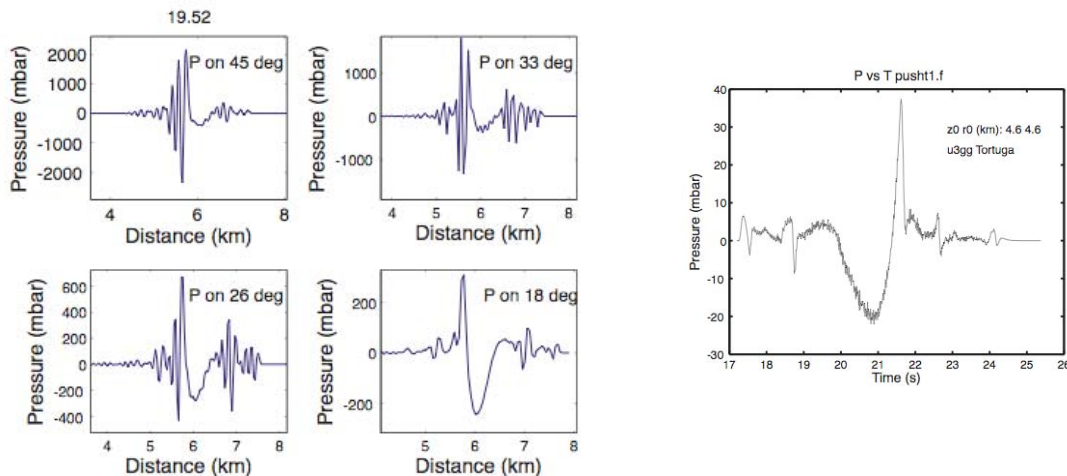

Figure 8. A comparison of CAVEAT and RI code results for the Tortugas, U3gg, event. The left four panels are CAVEAT profiles at 20 seconds. The CAVEAT results are for the finer zoned calculation. The right plot is the RI code result at 45 degrees and range of 6.5 km. Due to a plotting error, the RI code pressures should be a factor of 10 larger.

Some Analytic Considerations

1. An obvious direction in this work is that of a Fourier approach to the RI formulation. This is would serve as an easy way to compute the radiation pattern of ground-motion sources. A nice approach was given by Wecksung (1985) in an unpublished report and is summarized below for ease of reference, with some notational changes. The basic integral is given by

$$p(\vec{R},t) = \frac{\rho_0}{2\pi} \iint_A \frac{a(x,y,t-r/c)}{r} dxdy \cdot \qquad (2)$$

The area of motion is smaller than R_0, the distance from the center of the motion to the observation point. The source point on the ground is at $r_0 = r_0(x,y,0)$, and r is the distance from the source point to the observation point R. It is possible to use $1/R_0$ for the $1/r$ term in the integral and take it outside. Apply a change of variable of $\tau = t-r/c$ and take a temporal Fourier transform of Eq. (2) to get

$$\hat{p}(\vec{R},\omega) = \frac{\rho_0}{2\pi R_0} \iint_A \int_{-\infty}^{\infty} (a(x,y,\tau)dxdy)e^{-i2\pi\tau}d\tau e^{-i2\pi r/c} \cdot \qquad (3)$$

The normal acceleration, a, is related to the normal velocity, u, by

$$a(x,y,t) = \frac{\partial u(x,y,t)}{\partial t}, \qquad (4)$$

and the integral over $a(x,y,t)$ becomes

$$\int_{-\infty}^{\infty} a(x,y,\tau)e^{-i\omega\tau}d\tau = i\omega\hat{u}(x,y,\omega), \qquad (5)$$

where we have replaced $2\pi f$ with ω and $\hat{u}$ is the temporal Fourier transform of u. Then using Eq. (5), we can write

$$\hat{p}(\vec{R},\omega) = \frac{i\omega\rho_0}{2\pi R_0} \iint_A \hat{u}(x,y,\omega)e^{-i\omega r/c} dxdy \cdot \qquad (6)$$

At this stage the basic acceleration integral has been transformed, through a temporal Fourier transform, to a spatial Fourier transform of the normal velocity transform. Next, let e be a unit vector in the direction of R, $\hat{e} = (\sin\theta\cos\phi, \sin\theta\sin\phi, \cos\theta)$. It is possible to write $\vec{r} = \vec{R} - \vec{r}_o$ and from that, have $r^2 = R^2 - 2\vec{R}\cdot\vec{r} + r_0^2$. A little simplification gives an approximate expression for r, $r \approx R - (x\sin\theta\cos\phi + y\sin\theta\sin\phi)$. Next, for the spatial transform of $\hat{u}$, write

$$U_\omega(\upsilon_x,\upsilon_y) = \iint_S \hat{u}(x,y,\omega)\exp[-i2\pi(x\upsilon_x + y\upsilon_y)]dxdy, \qquad (7)$$

and with the approximate expression for r, Eq. (6) may be rewritten as

$$\hat{p}(\vec{R},\omega) = \frac{i\omega\rho_0}{2\pi R} \exp(-\frac{i\omega R}{c})U_\omega\left(\frac{-\omega\sin\theta\cos\phi}{2\pi c}, \frac{-\omega\sin\theta\sin\phi}{2\pi c}\right) \cdot \qquad (8)$$

The acoustic intensity is related to the pressure by

$$I_\omega(\vec{R}) = \frac{\left|\hat{p}(\vec{R},\omega)\right|^2}{\rho_0 c}, \qquad (9)$$

which leads to an expression for the far field intensity

$$I_\omega(\vec{R}) = \frac{\rho_0\omega^2}{4\pi^2 R^2 c}\left|U_\omega\left(\frac{-\omega\sin\theta\cos\phi}{2\pi c}, \frac{-\omega\sin\theta\sin\phi}{2\pi c}\right)\right|^2 \cdot \qquad (10)$$

918

2. Below is given a simple and straightforward derivation of an expression for the maximum amplitude of a uniform piston. Let the piston displacement be given by

$$z = A\sin(2\pi ft),$$ (11)

where A is the amplitude of the motion, f is frequency, and t is time. Then the velocity is given by

$$V = 2\pi fA\cos(2\pi ft).$$ (12)

On axis, the solution for pressure from an uniform piston is proportional (Pierce 1989) to a difference of velocities at retarded times,

$$p(h) = \rho c\left[V(t - \frac{h}{c}) - V(t - \frac{\sqrt{h^2 + R^2}}{c})\right] = \rho c\Delta V,$$ (13)

where h is the height above the center of the piston, R is the radius of the piston, ρ is the air density, and c is the speed of sound. From Eq. (12), the ΔV term can be written as

$$\Delta V = Aa\left[\cos(a(t - \frac{h}{c})) - \cos(a(t - \frac{\sqrt{h^2 + R^2}}{c}))\right],$$ (14)

where $a = 2\pi f$. We assume $h \gg R$, then the square root term becomes

$$\frac{h}{c} + \frac{R^2}{2ch} = \frac{h}{c} + y$$ (15)

Let $(t-(h/c)) = b$, substitute Eq. 15 in Eq. 14, expand the second cosine term, cancel obvious terms and use the small angle approximations for sine and cosine to get

$$\Delta V = -Aa^2 y\sin(ab),$$ (16)

with a maximum of Aa^2y. Then Eq. (13) can be rewritten as (for the maximum value)

$$p(h) = \rho cAa^2 y = \frac{2\pi^2 A\rho f^2 R^2}{h}.$$ (17)

Evaluation then requires only the displacement amplitude, frequency, piston radius, air density and altitude. An equivalent expression to Eq. (17) was given, without derivation, in Banister (1979) but had been overlooked by the author.

Some Additional Items

Ground-motion data, from measured ground-motion data files, for the 30 modeled events have been extracted. The accelerations and velocities plots have been put into a draft report that can be supplied upon request. Power spectra are now routinely computed for any case calculated by the RI code. A postprocessor was written to extract radial slices from the CAVEAT mesh.

CONCLUSIONS AND RECOMMENDATIONS

The improved velocity model from the RI code input to CAVEAT was implemented just before the deadline for the submission of this paper; only a few runs have been made. The mesh resolution in the CAVEAT runs needs further exploration. Initial comparisons of CAVEAT profiles with the RI code show some differences that need to be studied and understood.

REFERENCES

Addessio, Frank L., John R. Baumgardner, John K. Dukowicz, Norman L. Johnson, Bryan A. Kashiwa, Rick M. Rauenzahn, and Charles Zemach (1992). CAVEAT: A computer code for fluid dynamics problems with large distortion and internal slip, Los Alamos National Laboratory technical report, LA-10613, Rev. 1.

Banister, J. R., A program for predicting ground motion induced air pressures (1979). Sandia National Laboratories report SAND 78-2361.

Jones, Eric M., Frederick N. App, and Rodney W. Whitaker (1993). Ground motions and the infrasound signal: A new model and the discovery of a significant cavity rebound signal, Los Alamos National Laboratory technical report LA-UR 93-861.

Lee, Huan and James J. Walker (1980). Model for ground motion and atmospheric overpressure due to underground nuclear explosions, Los Alamos Scientific Laboratory report LA-8554-MS.

Mutschlecner, J. Paul and Rodney W. Whitaker (2005). Infrasound from earthquakes, *J. Geophys. Res.* 110: D01108, doi:10.1029/2004JD0050067.

Pierce, Allan D. (1989). *Acoustics, an Introduction to Its Physical Principles and Applications*. New York: Acoustical Society of America.

Press, William H., Brian P Flannery, Saul Teukolsky, and William T. Vetterling (1990). *Numerical Recipes (Fortran Version)*. Cambridge University Press.

Wecksung, George W. (1985). Acoustic radiation patterns associated with the ground motion produced by a contained nuclear explosion, Amparo Corporation report (unpublished).